

Influence of Additional Sr and TiB on Aluminium Al-Si-Cu-Mg Alloys for Produced Prototype Cylinder Head Motorcycle

Suherman^a, Syakura, A. ^bPanjaitan, A^c. Amirsyam^d. Mizhar, S^eA.Handoko^f

^{a,b,c}) Department of Mechanical Engineering, Polytechnic of Tanjungbalai, Indonesia

^d) Department of Mechanical Engineering, Medan Area University, Indonesia

^{f,g}) Department of Mechanical Engineering, Medan Institute of Technology, Indonesia

*Corresponding author: suherman.me.poltan@gmail.com

Paper History

Received: 15-September-2018

Received in revised form: 25-September-2018

Accepted: 4-October-2018

ABSTRACT

Lost-foam casting is a cast method that uses expanded polystyrene foam (EPS) as a mold pattern embedded into silica sand. At this foundry the cooling rate of molten metal is slowly, affecting the size of silicon particles and mechanical properties. The aim of this work is to investigate the effect of addition modifier Sr and Grains refiner to hardness, toughness, tensile strength and microstructure of A319. The mold pattern EPS foam prototype cylinder head pinned in silica sand. The aluminum A319 was melted in a furnace and poured at a temperature of 700 °C. The experimental results showed additional Sr or TiB increase the tensile strength and toughness of the cast, but not significantly affect the hardness of the casting.

KEYWORD: A319, modifier Sr, grain refiner TiB, Lost Foam Casting, cylinder heads

1.0 INTRODUCTION

The Lost foam casting is casting method that uses the patterns (EPS) of polystyrene foam. The method could have make the casting with complex and complicated shape, this method also has advantages is the flexibility of pattern. The prototype of casting product would be done fast by this casting method, lately, it has become the method for the manufacture of a part automotive component with mass production. Automotive components such as cylinder block, cylinder heads can be made by foam pattern method.

Chemical elements used to control the morphology of silicon particles and can change microstructure are called

modifiers [1]. Generally, the addition of Sr and Na as modifiers in Al-Si alloys to produce eutectic silicon structures with fibrous shapes [1].

The grain size of aluminum alloy depends on the number of grains formed in molten metal before the start of freezing and under cooling. The addition of several elements into the liquid metal can promote the initial formation of the nucleus and would be growth develop grains. The optimum number of TiB grains added up by 0.17% [2]. The additional grain refiner TiB in Aluminium A319 Alloys is important for improve mechanical properties such as hardness and tensile strength, reduce amount porosity, resistant hot cracking, change microstructure and improve the casting surface [1]. There is kind of newly introduced grain refiners such as TiB and TiC. Generally, in Al-Si alloys are added TiB grains as inoculants [3].

Research on the lost foam casting of aluminum A319 Alloys have been by several researchers [4]; [5]; [6]; [7]. The research on other materials was also reported [8,9,10,11,12,13]. The lost foam casting has a deficiency as the mount porosity [14], grain size and SDAS greater than silicon particles [14], hardness values and tensile strength are also lower [14] lower density [9], flap defects, blisters. the casting method that cooling rate of liquid metal occurs lower caused morphology eutectic silicone acicular shape and eutectic silicon more than roughness[4].

Therefore with the addition of TiB grain refiner and Sr modifier improve mechanical properties such as hardness and tensile strength of Al-Si-Cu-Mg aluminum alloy (A319) used to make prototype cylinder head motorcycle 2 stroke

2.0 MATERIALS AND METHODS

The Material is used this research Aluminium ingot commercial A319 with such composition (Table 1). The pattern polystyrene of prototype cylinder head was cut used hot wire up to an accuracy of ± 1 mm with a density of 20 Kg / m³. The cylinder head pattern is coupled with a runner and then dipped into a Zircon slurry (ZR-A) and colloidal silicate during 60 seconds (Figure 1).

The Silica sand used in this study is with mesh 60-80. The polystyrene pattern is placed at the bottom of the flask, and the flask is filled with silica sand with vibration.

Table 1 Chemical Composition Al-Si-Cu-Mg (mass %)

Si	Fe	Mg	Mn	Cu	Zn	Pb	Ca	Cr
8.28	0.94	1.4	0.534	2.1	0.5	0.1	0.02	0.06

Master alloy Al-5Ti-1B is added in a molten aluminum A319 alloys with concentrations range from 0.1 wt%. Measurement of molten metal temperature was using thermocouple type-K. Aluminum A319 alloy melted at 750 °C and poured at temperature 700°C surface polystyrene pattern. The composition of each alloy is measured by an optical emission spectrometer. The microstructural observations were performed on the base and cylinder head fins. Tensile test bars and impact specimen tests are carried out from the base of the cylinder head cast. The tensile test bar is made following the ASTM E-801 standard. The Impact test specimens were carried out following the ASTM E-23 standard using the Charpy test machine method.

The fracture surface of the charpy test specimen was also examined for morphology with Scanning Electron Microscopy (SEM), coupled with energy-dispersive X-ray spectroscopy (EDX). The hardness of the test results compared with the hardness value between the fin and base parts was tested by the Rockwell Hardness method. The value of the hardness of the specimen was taken randomly at least five measurements of each sample and averaged to obtain the hardness value of the specimen. The Optical microscope is used to obtain qualitative data of castings before and after the addition of Srontium as modifier Si Particle and TiB grain refiner. Phase identification is also done by X-ray diffraction method (Zeiss).

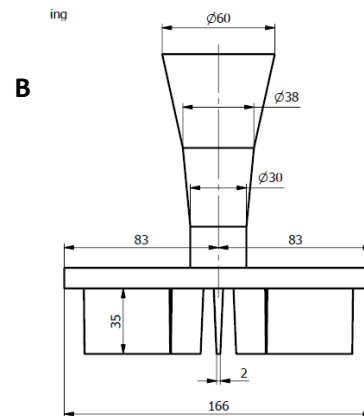
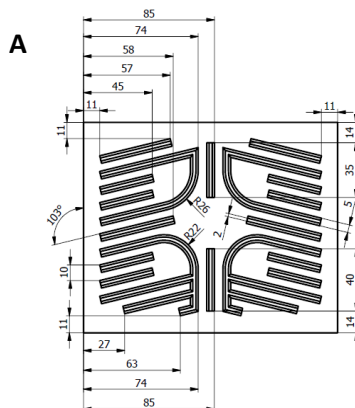


Figure 1. Pattern LFC of cylinder head a) top view b) side view

3.0 RESULT AND DISCUSSION

The cast aluminum alloy A319 is studied with an optical microscopy as shown in Fig. 2. The microstructure of Aluminum A319 alloys is influenced by iron content, silicon, magnesium and copper in the alloy. The iron content in aluminum alloy generally damages the mechanical properties because of its intermetallic phase of β -Al-Fe-Si intermetallics with a plate-like form found at grain boundaries. The Microcrack initiation generally occurs in the β -Al-Fe-Si region and is also enhanced by micropores[5]. The amount of Mn content in A319 alloy forms a morphology commonly called Chinese script [4]. According to [6] the intermetallic structure of iron have distinguished become 2 especially the α phase (AlFeMnSi) with structures known as "Chinese script" and β (AlFeSi) phases in platelets.

The silicon is usually added to aluminum as the main matrix in aluminum because it has the properties to castability and fluidity. Silicon particles show a plate-like (acicular shape). The cooling rate most affects morphology of silicon particles. Eutectic silicon particles are not evenly dispersed with shorter plate forms, this possible due to faster cooling rate result in fast solidification time as reported [10]. The pouring temperature also influence the length of silicon particles, enhance the liquid metal pour temperature increases the particle size of the silicon [15].

All of the intermetallic copper in aluminum alloy crystallizes at the end of solidification in the remaining dendritic fluid. The Ω -Al₂Cu phase appears in A319 as a eutectic bag mixed with an aluminum matrix. Al₂Cu phase is observed, forming a block between the eutectic Si phase and the intermetallic phase[6]. Morphology the β -Mg₂Si phase of small black develops in the final stages of solidification with a very high cooling rate. the only Amount β -Mg₂Si phases are observed in the microstructure because the LFC cooling rate is very low [4]. the microstructure observation (figure 2) aluminum A319 alloys casted by the LFC method shows a slightly rough Secondary Dendrite Arm Spacing (SDAS) approximately 70-80 μ m [16]. SDAS size is very strongly influenced by the rate of cooling, besides that the chemical composition also affects the characteristics of microstructure.

The observation with SEM as shown in figure 3, the porosity of the irregularly shaped cast objects is scattered on the castings. The number Porosity cast metal increase with the pouring temperature enhance, but surface roughness enhance with increase of pour temperature [15]. Large porosity size is the initiation of crack when first tensile loading is performed and growth along inclusions such as the silicon phase, intermetallic iron, and copper phase[17].

3.1. Microstructure As Cast

The observations used SEM appear forms are brittle fractures as reported [4]. The addition of Sr to the A319 alloy increases the ductility of the castings in which the fracture appears cup and cone [4]. Study of cracked surfaces was performed on the surface of the impact test sample. The A319 alloyed impact sample shows the fracture mechanism occur during the impact testing of the alloy.

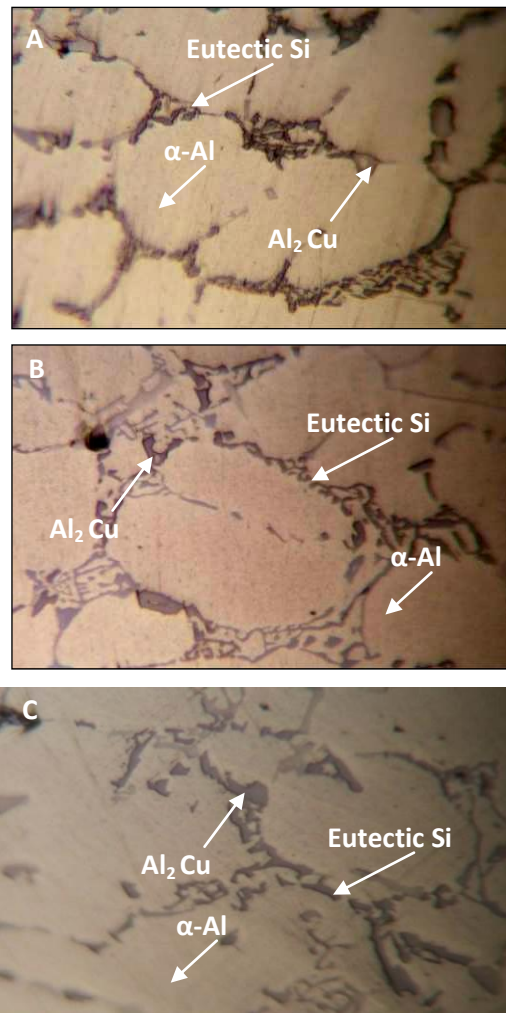
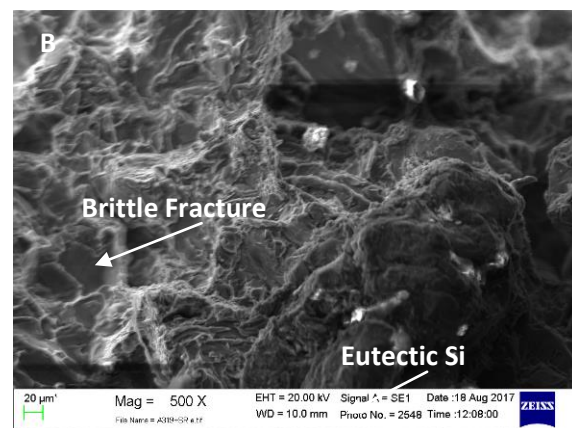
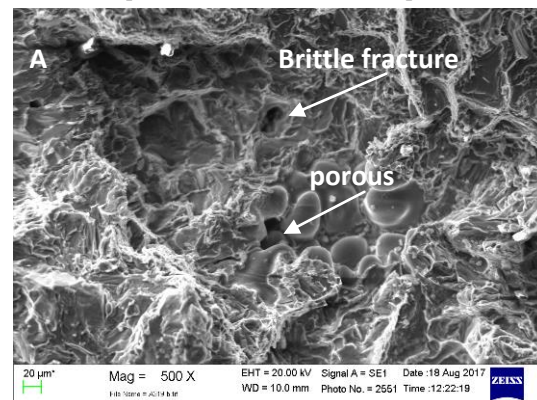


Figure 2 microstructure of cast A319 a) un-modification b) A319 grain refiner TiB dan c) A319 addition Sr

Figure (3.a) shows morphology surface of Al-A319 alloy fracture with lost cast foam casting (LFC) casting method. The Fracture surfaces show several intermetallic phases including Al₂Cu and Si particles obtain in cast alloy A319. It is generally the fractured form is dominated by the brittle fracture of the Al₂Cu phase, the intermetallic phase, and the silicon particles, in addition, oxygen concentrations are also seen in A319 alloys using EDX measurements (see Figure 2a) at locations marked with red lines in the image 2.a). this confirms that the pores always appear along with the film oxide that can facilitate the nucleation of the pores. All the fracture surfaces show a mixed mode of ductile fracture and brittle fracture (figure 3 b).

Figure (3.c) shows the brittle fracture of the sample as evidenced by the long size Si particle fracture (see red arrow in Figure 3.c) in A319 alloy. Crack propagation observed occurs between dendritic, except that blocky Al₂Cu occurring blocky of molten aluminum melting during solidification is also responsible for fracture surfaces. Aluminum A319 without the addition of Strontium it is seen that the crude planar fracture surface represents the fracture region in the cleavage of the silicon particle region. Porosity is also present in the A319 alloy in the cast by the method of lost foam casting which is responsible for the occurrence of stress concentration when the impact test is done. This matter the porosity occurs when the polystyrene foam is decomposed by the molten aluminum when the liquid aluminum fills the mold pattern



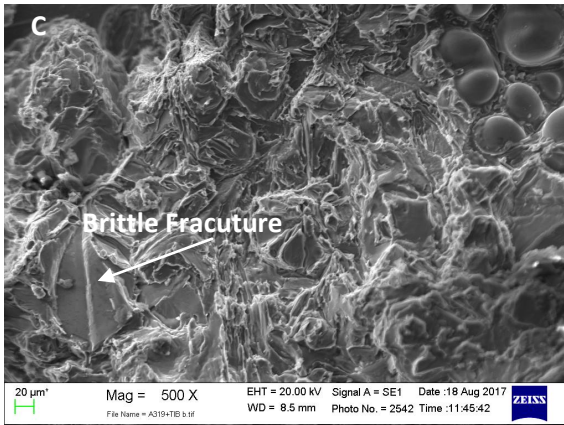


Figure 3 SEM low magnification fracture morphologies of A319 Impact Specimen a) un-modification b) Additional Sr and c) additional TiB

The modified Al-A319 alloy with Strontium shows the various intermetallic phases of Si particles found on the surface of the fracture of the particle impact test. The sample appears to be composed of repetitive structures (Figure 2.c). In addition, α -Al looks more dominant in the A319 alloys that have been added Sr. In the A319 alloys that have been added Sr using EDX measurements also shows that the oxygen concentration is found. This occurs because of the turbulent flow that occurs during the pouring of molten aluminum into the mold cavity.

The modified Al-A319 alloy fractography with Sr shows the various intermetallic phases of Si particles found on the surface of the fracture of the particle impact test. The sample appears to be composed of repetitive structures (Figure 2.c). In addition, α -Al looks more dominant in the A319 alloys that have been added Sr. In the A319 alloys that have been added Strontium using EDX measurements also shows that the oxygen concentration is found. This occurs because of the turbulent flow that occurs during the pouring of molten aluminum into the mold cavity. A finer fracture surface in the deformed region occurs in the Al matrix. The smoother surface of the fracture indicates that the fracture occurs in a more resilient manner than the A319 alloy without modification. In this case, it indicates that Sr as a modifier renders the rough silicon structure to a finer silicon structure (Fig. 2.c)

3.2. MECHANICAL PROPERTIES

Table 2 Mechanical Properties Aluminium A319 Alloy

Materials	UTS (Mpa)	Impact (J/mm ²)	Hardness (HRB)
A319	110	0.40	79
A319 + TiB	124	0.74	82
A319+Sr	144	0.76	82

Table 2 shows the mechanical properties of casting Aluminium A319 Alloys prototype cylinder head. The addition of Sr and TiB to the aluminum alloy affects mechanical properties such as hardness, tensile strength, and toughness. The mechanical properties of casting increase especially at

maximum tensile strength and toughness but not significantly on hardness value.

4.0 CONCLUSION

In this study, microstructure and mechanical properties of A319 aluminium alloys modified Strontium and grain refiner TiB were investigated and compared. The addition of TiB grain and Sr on aluminum A319 alloy increase the tensile strength and toughness of castings but insignificantly affect the hardness of cast. Aluminum A319 Alloys are cast using the lost foam method (LFC) form silicone particles Chinese script

ACKNOWLEDGMENTS

The authors gratefully acknowledge the contribution of the financial support of the Ministry Ristekdikti of Indonesian No 119/K1.1/LT.1/2017 and Polytechnic of Tanjungbalai, Medan Institute of Technology for providing research facilities.

REFERENCE

1. J. Brown, *Foseco non-ferrous foundryman's handbook*. Butterworth-Heinemann, 1999.
2. S. G. Shabestari and M. Malekan, "Assessment of the effect of grain refinement on the solidification characteristics of 319 aluminum alloy using thermal analysis," *J. Alloys Compd.*, vol. 492, no. 1–2, pp. 134–142, Mar. 2010.
3. J. R. Davis, *ASM Specialty Handbook: Heat-Resistant Materials*. ASM International, 1997.
4. S. Tabibian, E. Charkaluk, A. Constantinescu, A. Oudin, and F. Szymtka, "Behavior, damage and fatigue life assessment of lost foam casting aluminum alloys under thermo-mechanical fatigue conditions," *Procedia Eng.*, vol. 2, no. 1, pp. 1145–1154, Apr. 2010.
5. S. Tabibian, E. Charkaluk, A. Constantinescu, F. Szymtka, and A. Oudin, "TMF-LCF life assessment of a Lost Foam Casting A319 aluminum alloy," *Int. J. Fatigue*, vol. 53, pp. 75–81, Aug. 2013.
6. N. Dahdahet *et al.*, "Influence of the Casting Process in High Temperature Fatigue of A319 Aluminium Alloy Investigated By In-Situ X-Ray Tomography and Digital Volume Correlation," *Procedia Struct. Integr.*, vol. 2, pp. 3057–3064, 2016.
7. L. Wang *et al.*, "Influence of pores on crack initiation in monotonic tensile and cyclic loadings in lost foam casting A319 alloy by using 3D in-situ analysis," *Mater. Sci. Eng. A*, vol. 673, pp. 362–372, Sep. 2016.
8. H. Jafari, M. H. Idris, and A. Shayganpour, "Evaluation of significant manufacturing parameters in lost foam casting of thin-wall Al-Si-Cu alloy using full factorial design of experiment," *Trans. Nonferrous Met. Soc. China*, vol. 23, no. 10, pp. 2843–2851, Oct. 2013.
9. W. Jiang, Z. Fan, D. Liao, D. Liu, Z. Zhao, and X. Dong, "Investigation of microstructures and mechanical properties of A356 aluminum alloy produced by expendable pattern shell casting process with vacuum and low pressure," *Mater. Des.*, vol. 32, no. 2, pp. 926–934, Feb. 2011.
10. A. A. Niakan, M. H. Idris, M. Karimian, and A. Ourdjini, "Effect of Pressure on Structure and Properties of Lost

- Foam Casting of Al-11Si Cast Alloy,” *Appl. Mech. Mater.*, vol. 110–116, pp. 639–643, Oct. 2011.
11. W. JIANG, Z. FAN, and D. LIU, “Microstructure, tensile properties and fractography of A356 alloy under as-cast and T6 obtained with expendable pattern shell casting process,” *Trans. Nonferrous Met. Soc. China*, vol. 22, pp. s7–s13, 2012.
 12. M. Karimian, A. Ourdjini, M. H. Idris, and H. Jafari, “Effects of Casting Parameters on Shape Replication and Surface Roughness of LM6 Aluminium Alloy Cast Using Lost Foam Process,” *Trans. Indian Inst. Met.*, vol. 68, no. 2, pp. 211–217, Apr. 2015.
 13. W. Jiang, Z. Fan, X. Chen, B. Wang, and H. Wu, “Combined effects of mechanical vibration and wall thickness on microstructure and mechanical properties of A356 aluminum alloy produced by expendable pattern shell casting,” *Mater. Sci. Eng. A*, vol. 619, pp. 228–237, Dec. 2014.
 14. W. Jiang, Z. Fan, X. Chen, B. Wang, and H. Wu, “Combined effects of mechanical vibration and wall thickness on microstructure and mechanical properties of A356 aluminum alloy produced by expendable pattern shell casting,” *Mater. Sci. Eng. A*, vol. 619, pp. 228–237, Dec. 2014.
 15. H. Jafari, M. H. Idris, and A. Shayganpour, “Evaluation of significant manufacturing parameters in lost foam casting of thin-wall Al–Si–Cu alloy using full factorial design of experiment,” *Trans. Nonferrous Met. Soc. China*, vol. 23, no. 10, pp. 2843–2851, 2013.
 16. Z. Li, N. Limodin, A. Tandjaoui, P. Quaegebeur, P. Osmond, and D. Balloy, “Influence of Sr, Fe and Mn content and casting process on the microstructures and mechanical properties of AlSi7Cu3 alloy,” *Mater. Sci. Eng. A*, vol. 689, pp. 286–297, Mar. 2017.
 17. N. Dahdahet *al.*, “Influence of the Casting Process in High Temperature Fatigue of A319 Aluminium Alloy Investigated By In-Situ X- Ray Tomography and Digital Volume Correlation,” *ProcediaStruct. Integr.*, vol. 2, pp. 3057–3064, 2016.